Chromophore Organization in the Higher-Plant Photosystem II Antenna Protein CP26

Roberta Croce, Giusy Canino, Francesca Ros, and Roberto Bassi*

Dipartimento Scientifico e Tecnologico-Facoltà di Scienze MM.FF.NN., Strada Le Grazie 15, 37134 Verona, Italy

Received February 27, 2002; Revised Manuscript Received April 12, 2002

ABSTRACT: The chlorophyll *a*/*b*−xanthophyll−protein CP26 complex belongs to the Lhc protein family. It binds nine chlorophylls and two xanthophylls per 26.6 kDa polypeptide. Determination of the characteristics of each binding site is needed for the understanding of functional organization of individual proteins belonging to the photosystem II supramolecular complex. The biochemical and spectroscopic features of native CP26 are presented here together with identification of pigment binding and energy transitions in different sites. The analysis has been performed via a new approach using recombinant CP26 complexes in which the chromophore content has been experimentally modified. Data were interpreted on the basis of homology with CP29 and LHCII complexes, for which detailed knowledge is available from mutation analysis. We propose that one additional Chl *b* is present in CP26 as compared to CP29 and that it is located in site B2. We also found that in CP26 three chlorophyll binding sites are selective for Chl *a*, one of them being essential for the folding of the pigment−protein complex. Two xanthophyll binding sites were identified, one of which (L1) is essential for protein folding and specifically binds lutein. The second site (L2) has lower selectivity and can bind any of the xanthophyll species present in thylakoids.

The Chl *a*/*b*−xanthophyll−protein complexes belong to the Lhc multigene family (*1*), providing components of the antenna system of higher plants. These are involved in two important aspects of photosynthesis: (i) light absorption and transfer of the excitation energy to reaction centers for charge separation and (ii) photoprotection mechanisms that involve thermal dissipation of excess Chl[1] *a**, aimed at preventing photoinhibition and photobleaching (*2*). Although a growing body of information about the mechanisms underlying both functions has recently been obtained (*3*, *4*), the precise understanding of structure−function relations is still far for being satisfactory. A model for the structure of Lhc proteins has been derived from electron crystallographic analysis of the major LHCII complex (*5*), revealing the organization of chromophores, which are bound to three transmembrane helices and a small amphiphilic helix. Two xanthophyll molecules have been shown to be cross-braced to helices A and B. Eight or nine Chl molecules appear to be coordinated to nucleophilic amino acid residues, while four or five additional Chls and two xanthophylls are held in place by interactions with other pigments. Further biochemical analysis yielded a total complement of eight Chl *a* molecules, five Chl *b* molecules, and four xanthophylls per polypeptide in the case of the major LHCII complex (*6*−*8*). Although Lhc proteins share a high degree of homology, differences can be recognized in both their polypeptide and chromophore moieties. Thus, phosphorylation sites have been found in Lhcb1, Lhcb2, and Lhcb4 gene products, although they are located in different positions within the N-terminal, stromally exposed, domain (*9*, *10*). Protonation sites, located on the lumenal loops of Lhcb4 (*11*) and Lhcb5 (*12*), have been detected by DCCD binding, which partially overlap Ca^{2+} binding sites (*13*). The chromophore composition of Lhc proteins is also variable. Chl/polypeptide ratios of 8 (Lhcb4), 9 (Lhcb5), 10 (Lhcb6 and LHCI), and 12 (Lhcb1) have been reported (*6*, *14*−*16*).

Purification of individual Lhc proteins from thylakoids is difficult due to their very similar physicochemical properties. This problem has been overcome by in vitro reconstitution of recombinant apoproteins overexpressed in bacteria (*17*−*19*), thus allowing functional studies on individual gene products.

Ultrafast spectroscopic measurements (*20*−*23*) yielded a detailed knowledge of the energy transfer processes (*24*) and of the effects of incorporating xanthophyll cycle pigments on the energy conservation and/or dissipation properties of Lhc proteins (*4*, *25*−*28*). Studies of Lhcb1 and Lhcb4 proteins by mutation analysis (*6*, *29*−*31*) showed that important spectroscopic (i.e., functional) differences between Lhc products are associated with the occupancy and/or vacancy of individual pigment binding sites and by the possibility of a particular site to be occupied by a different Chl or xanthophyll species.

In this work, we have studied the chromophore organization of CP26, the product of the nuclear gene Lhcb5, encoding a 247-amino acid polypeptide. This monomeric subunit is located between the CP43 subunit of the PSII

* To whom correspondence should be addressed. Telephone: 0039-045-8027916. Fax: 0039-045-8027929. E-mail: bassi@sci.univr.it.

[1] Abbreviations: Chl, chlorophyll; DCCD, dichlorocyclohexylcarbodiimmide; IEF, isoelectrofocalization; L, lutein; LT, low temperature; N, neoxanthin; nCP26, native CP26; NPQ, non-photochemical quenching; rCP26, recombinant CP26; RT, room temperature; V, violaxanthin; Z, zeaxanthin.

10.1021/bi0257437 CCC: $22.00
Published on Web 05/11/2002

reaction center and the S trimer of LHCII (*32*). Its primary structure is highly homologous to LHCII, thus suggesting a similar folding. Moreover, seven of eight Chl-binding residues in LHCII are conserved in CP26 but for the ligand of Chl in the B6 site, which is a glutamic acid rather than a glutamine, a characteristic shared with CP29. Nevertheless, CP26 binds nine Chls (six Chl *a* and three Chl *b* molecules) (*14*, *33*) and one Chl *b* in addition with respect to CP29. Lutein, violaxanthin, and neoxanthin are bound in a total of approximately 2 mol/mol of polypeptide (*34*, *35*), although a value of 3 was also reported for the spinach complex (*33*). An interesting question is whether violaxanthin is bound to a high-affinity site (*28*, *36*) or to a low-affinity peripheral site (*33*) similar to the V1 site in LHCII (*8*). This is relevant for the understanding of the mechanism of thermal dissipation due to the following findings: (i) CP26 binds zeaxanthin under high-light conditions (*37*) leading to fluorescence quenching (*28*), and (ii) it possesses two binding sites for the NPQ inhibitor DCCD (*38*), suggesting it can be active in xanthophyll cycle-mediated NPQ and may respond to a low lumenal pH.

We have studied CP26, either purified from leaves or recombinant. The affinity of pigment binding sites was probed by biochemical and spectroscopic analysis of complexes reconstituted in the presence of different ratios between chromophores. The results were interpreted by comparison with the properties of two homologous proteins, namely, CP29 and LHCII, the chromophore organization of which is known from previous work. As a result, we propose a model for the occupancy of chromophore binding sites in CP26.

MATERIALS AND METHODS

Purification of the Native Complex. Native CP26 (nCP26) was purified from a maize grana preparation (*39*) by IEF and sucrose gradient ultracentrifugation as previously reported (*40*).

Reconstituted Complex. The apoprotein was obtained as reported in ref *36*. The reconstitution and purification of the reconstituted complexes were performed as described in ref *19*. Complexes with a modified Chl *a*/*b* and carotenoid composition were obtained by changing either the Chl *a*/*b* ratio or the carotenoid species in the pigment mixes used for reconstitution.

Pigment Analysis and Pigment/Protein Stoichiometry. The pigment complement of the holoprotein was analyzed by HPLC (*41*) and fitting of the acetone extract with the spectra of the individual pigments (see below for a description of the fitting program).

The protein was quantified by ninhidrin method (*42*) and by SDS−PAGE analysis (*15*).

Spectroscopy. The absorption spectra at RT were recorded with an SLM-Aminco DK2000 spectrophotometer, in 10 mM Hepes (pH 7.5), 20% glycerol, and 0.06% DM. A 0.4 nm step was used. LT spectra were obtained as reported in ref *43*.

The fluorescence emission spectra were measured on a Jasco FP-777 fluorimeter in a 1 cm × 1 cm cuvette and corrected for the instrumental response. The samples were excited at 440, 475, and 500 nm. The bandwidths were 5 nm in excitation and 3 nm in emission. All fluorescence spectra were measured at 0.01 OD at the maximum of the Q_y transition.

LD spectra at RT and LT were obtained as described in refs *44* and *45* using samples oriented by the polyacrylamide gel squeezing technique. The measurements at the two temperatures were obtained on the same sample.

The CD spectra were measured at 10 °C on a Jasco 600 spectropolarimeter. The OD of the samples was 1 at the maximum in the Q_y transition for all complexes, and the samples were in the same solution described for the absorption. The measurements were performed in a 1 cm cuvette. All the spectra presented were normalized to the same polypeptide concentration, based on the Chl binding stoichiometry (*46*).

Denaturation temperature measurements were performed by following the decay of the CD signal at 679 nm when increasing the temperature from 20 to 80 °C with a time slope of 1 °C/min and a resolution of 0.2 °C. The signal (CD vs *T*) was fitted with a sigmoid function.

Data Analysis. The spectra of the acetone extracts of the protein were recorded in the visible range from 350 to 750 nm with the SLM-Aminco DW 2000 spectrophotometer as described above. The following procedure was used to fit the experimental spectra in terms of pigment spectral forms. (a) A library of spectra of pure pigments (Chl *a*, Chl *b*, lutein, neoxanthin, violaxanthin, and zeaxanthin) was obtained by recording spectra of pure pigments in 80% acetone. (b) These spectra were combined to obtain a fit of the spectrum of the acetone extracts from pigment−protein complexes by using homemade software based on Microsoft Excel and Visual Basic utilities. The software used the "solver" module of Excel to find first the least-squares solution of the polynomial combination that best fit the spectrum in the 600−750 nm region, thus determining the Chl *a*/*b* ratio. Once a satisfactory fitting in this region where only Chls absorb was obtained, the xanthophyll content was determined via the difference spectrum (original spectrum − Chl *a*+*b* calculated spectrum) in the Soret region (410−510 nm). To choose between possible nonunique solutions (because of the similarity of the absorption spectra of xanthophyll species), only solutions fitting the HPLC-determined ratio between xanthophyll species were accepted.

The same software has been adapted to fit the absorption spectra in the Q_y region of holoproteins. Spectral forms of Chl *a* and Chl *b* in the Lhc protein environment (*47*) were used instead of 80% acetone spectra. In the description of CP26 spectra, nine absorption forms were used, three Chl *b* and six Chl *a* molecules, in agreement with the pigment/polypeptide stoichiometry. In all cases, the Chl *a*/*b* ratio calculated from the fitting was in agreement with the value obtained from pigment analysis within 0.05.

RESULTS

Native CP26 Complex. The CP26 complex was purified from maize thylakoids by preparative IEF and sucrose gradient ultracentrifugation (*40*). When analyzed by SDS−PAGE, the preparation exhibited a single Coomassie-stained band at ∼28 kDa. Pigment content was determined upon extraction with buffered 80% acetone, and analysis was carried out by a combined approach of HPLC and fitting of the spectrum of acetone extracts with the spectra of individual

Table 1: Pigment Content of Samples with Different Chl *a*/*b* Ratios[a]

sample	Chl *a*/*b* mix[b]	Chl *a*/*b*	Chl *a*	Chl *b*	Neo	Viola	Lute	Chl tot	Chl/car
nCP26	−	2.2 ± 0.05	6.2	2.8	0.61	0.38	1.02	9	4.5 ± 0.1
rCP26-2.7	8	2.71 ± 0.05	6.57	2.43	0.72	0.32	0.97	9	3.9 ± 0.04
rCP26-2.25	5.5	2.25 ± 0.05	6.23	2.77	0.77	0.3	0.96	9	4.0 ± 0.1
rCP26-2.08	3	2.08 ± 0.04	6.08	2.92	0.76	0.3	1.04	9	4.1 ± 0.1
rCP26-1.7	1	1.7 ± 0.05	5.7	3.3	0.7	0.3	0.9	9	4.3 ± 0.05
rCP26-1.1	0.3	1.11 ± 0.04	4.7	4.28	0.7	0.3	0.9	9	4.2 ± 0.2
rCP26-0.23	0.05	0.23 ± 0.01	1.4	5.6	0.58	0.24	1.11	7[c]	3.1 ± 0.06
rCP26-0.11	<0.01	0.11 ± 0.01	0.7	6.3	0.64	0.3	1.08	7[c]	3.06 ± 0.06

[a] The samples were named after the values of the Chl *a*/*b* ratio in the reconstituted complex. The data presented are the averages of three measurements. For the pigment/protein ratio, samples nCP26 and rCP26-2.08 were analyzed by ninidrin methods over five repetitions, while for all other complexes, the protein concentration was determined by gel analysis over four repetitions. The maximum error was ±0.3. [b] Chl *a*/*b* used in the reconstitution mixture. [c] Based on the car content.

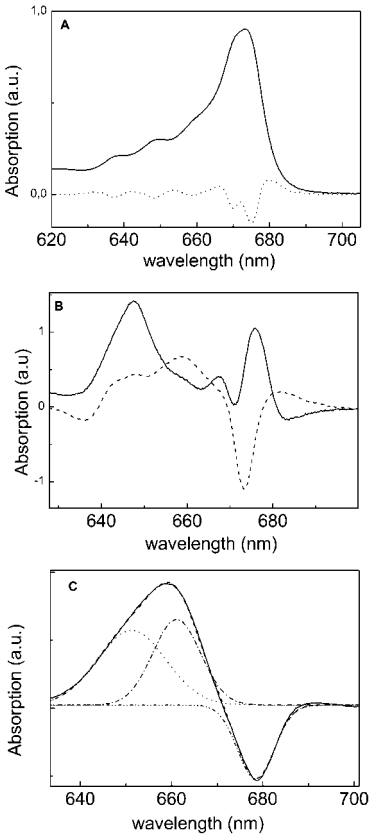

FIGURE 1: (A) Absorption spectrum (—) and its second derivative (···) of nCP26 at 10 K. (B) LHCII − CP26 (—) and CP26 − CP29 (···) difference spectra at 10 K. (C) CP26 − CP29 difference spectrum at RT and Gaussian deconvolution. Before subtraction, all absorption spectra were normalized to protein concentration.

pigments in this solvent (Table 1) (*48*). Pigment/protein ratio determination on native CP26 (nCP26) yielded a figure of 9 Chls per polypeptide, in agreement with previous data (*14*). Thus, nCP26 binds 6.2 Chl *a* molecules, 2.8 Chl *b* molecules, and 2 xanthophylls. The xanthophyll moiety included three species: lutein, violaxanthin, and neoxanthin in a 1:0.3:0.7 ratio.

The absorption spectrum and the second-derivative analysis of nCP26 at 10 K are reported in Figure 1. Minima are located at 637.4, 648.2, 659, 670, and 675 nm, where the first two can be attributed to Chl *b* Q_y transitions and the last two to Chl *a* molecules. The absorption spectrum of nCP26 was compared to the spectra of nCP29 and nLHCII, after normalization on the basis of the chromophore content and Chl *a*/*b* ratio (*46*), for identification of the spectral

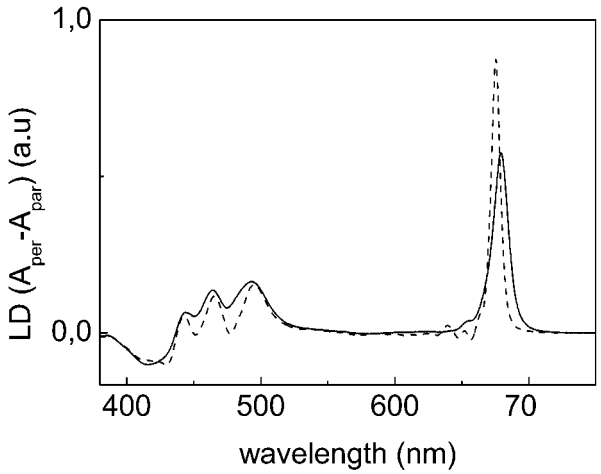

FIGURE 2: Linear dichroism spectra at 293 (—) and 10 K (···) of nCP26.

features associated with the difference in pigment content. Highly purified LHCII binds seven Chl *a* and five Chl *b* molecules (*14*). The nLHCII minus nCP26 difference spectrum at 10 K (Figure 1B) shows two major positive contributions at 647 and 676 nm. According to the pigment analysis, these spectral differences are likely to represent the energy levels of the Q_y transitions of the two Chl *b* chromophores and one Chl *a* chromophore lacking in nCP26 with respect to nLHCII. Minor contributions to the difference spectrum are also detected at 667 and 658 nm. nCP29 has six Chl *a* and two Chl *b* molecules (*14*), thus one fewer Chl *b* than nCP26. Their difference spectrum at LT (CP26 − CP29) shows a positive Chl *b* contribution at 647 nm which can readily account for the additional Chl *b* of CP26. However, two contributions of opposite sign [660 (+) and 673.5 nm (−)] are also resolved, suggesting that the absorption of at least one Chl *a* chromophore is blue-shifted in nCP26 compared to that in nCP29. The same components can be resolved at RT, although deconvolution is needed to appreciate the individual components at 651 (+), 662 (+), and 679 nm (−) (Figure 1C).

Linear dichroism spectra of nCP26 at RT and 10 K are shown in Figure 2. They are characterized by a large positive signal in the Chl *a* region (maxima of 675.4 nm at 10 K and 679.2 nm at 296 K). In the Chl *b* Q_y region (630−655 nm), the spectrum at RT is featureless, while small negative and positive contributions are observed at LT as previously reported (*43*). A similar behavior was previously reported in the case of nCP29 and shown to be due to the presence of multiple absorption forms, closely spaced in energy,

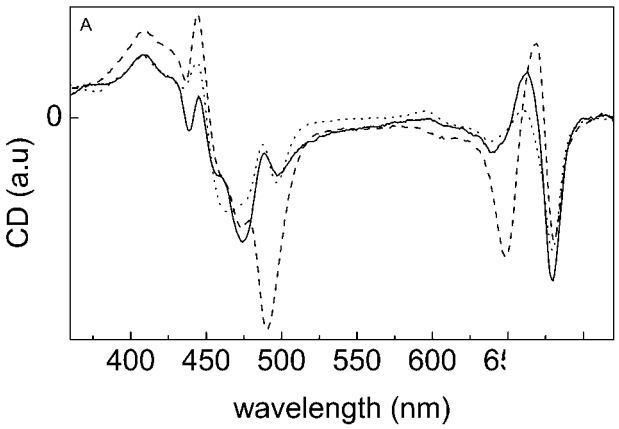

FIGURE 3: Circular dichroism spectra at 10 °C of nCP26 (—), nCP29 (•••), and nLHCII (- - -). The spectra were normalized to protein concentration.

originating from the partial occupancy by Chl *b* versus Chl *a* of four binding sites. The different orientation of their transition moments with respect to the membrane plane was shown to yield averaging of the LD signal around the zero line (*49*). It is thus likely that in CP26 the 2.8 Chl *b* molecules per polypeptide are distributed among several (four to five) binding sites. An alternative explanation, that the transition moments of all Chl *b* chromophores are oriented at the magic angle, is more unlikely, although cannot be ruled out. In the Soret region, a positive LD signal, peaking at 495 nm, can be attributed to xanthophyll absorption, while the positive contributions at 466 and 443 nm originate from the convolution of carotenoids and Chl *b* spectra. The negative signal at 430 nm is associated with Chl *a*.

In Figure 3, the circular dichroism spectrum of nCP26 is reported along with the CD spectrum of nCP29 and nLHCII. The spectra are normalized to the same protein concentration, as determined from the absorption of the samples in the Q_y region, according to the Chl/protein ratio of the complexes. In the 600−720 nm range, the spectra present two negative signals (640 and 680 nm) and one positive (663 nm) signal. The red-most (680−682 nm) signal is similar in the three spectra, while the amplitude of the 640 nm (−) signal is much higher in LHCII with respect to nCP29 and nCP26. The 663 nm (+) signal has the highest amplitude in nLHCII, while it is close to the zero line in CP29 and has intermediate amplitude in nCP26. In the Soret range, the spectra are complicated by the superimposition of the Chl and xanthophyll contributions. Striking is the difference in amplitude of a 491 nm (−) signal, attributed to the neoxanthin in LHCII since it is lacking in the absence of this xanthophyll species (*7*). This signal is both much smaller (1/8) and shifted (to 497 nm) in CP26 and CP29, thus suggesting a different organization of neoxanthin in LHCII with respect to CP29 and CP26.

Recombinant CP26 Proteins. To analyze in detail the source of biochemical and spectroscopic features of the CP26 complex, we have studied the effect of experimental modification of the chromophore content in rCP26 by refolding the apoprotein, overexpressed in *Escherichia coli*, in the presence of different chromophore complements. First, we changed the Chl *a*/*b* ratio in the reconstitution mixture; second, we performed the refolding in the presence of individual xanthophyll species or combinations of two.

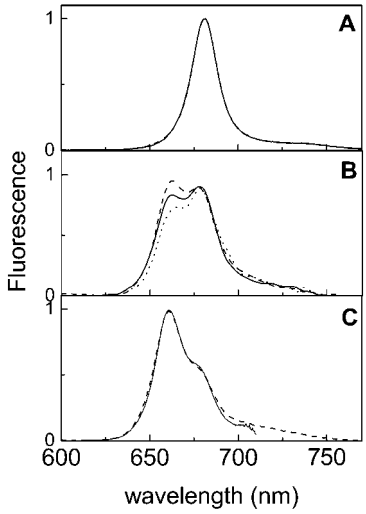

FIGURE 4: Fluorescence emission spectra at RT of complexes with different Chl *a*/*b* ratios following excitation at 440 (—), 475 (•••), and 500 nm (- - -): (A) rCP26-2.08, (B) rCP26-0.23, and (C) rCP26-0.11. In panel C, only the 500 nm spectrum and the Stepanov analysis (solid) are reported. All spectra are normalized to the maximum.

Chl a and Chl b. rCP26 was reconstituted in the presence of a range of Chl *a*/*b* ratios, from 0 to 10 in the pigment mix. Stable pigment−protein complexes were obtained in all cases except when Chl *b* was the only Chl species present in the reconstitution mix, an indication that Chl *b* alone is not able to sustain the folding process. Reconstitution in the presence of limiting amounts (traces) of Chl *a* (sample rCP26-0.11) showed a strong decrease in the yield of the pigment−protein complex. The recombinant complex thus obtained contained at least one molecule of Chl *a*. The decreased reconstitution yield of this complex is related to Chl *a* availability. We conclude that the binding of at least one Chl *a* per polypeptide is required for protein assembly.

The pigment composition of the reconstitution products is reported in Table 1. A Chl *a*/*b* ratio of 3 in the pigment mix was required to obtain a complex with the same pigment complement as the native protein. By decreasing the amount of Chl *a* available for the reconstitution, we obtained a complex with only seven rather than nine Chls, implying that two of the binding sites in CP26 are specific for Chl *a* but not essential for the stability of folding.

In all recombinant complexes, lutein was consistently bound in a ratio of one molecule per polypeptide while violaxanthin and neoxanthin together accounted for an additional one. The carotenoid composition of these samples is similar, implying that there is no preferential role for Chl *a* versus Chl *b* in determining the selectivity of xanthophyll binding to CP26.

Fluorescence emission spectra of rCP26 with different Chl *a*/*b* ratios were recorded following excitation at 440, 475, and 500 nm, selective for Chl *a*, Chl *b*, and xanthophylls, respectively. A selection of the spectra is shown in Figure 4. The spectral shape was independent of excitation wavelength, indicating efficient energy transfer between pigments. This is the case for all complexes with a Chl *a*/*b* ratio from 2.7 to 1.1 (data from rCP26-2.08 are shown in Figure 4A as representative data). In the case of rCP26-0.23, a slight wavelength dependence was detected (Figure 4B). We attribute this feature to sample heterogeneity rather than to

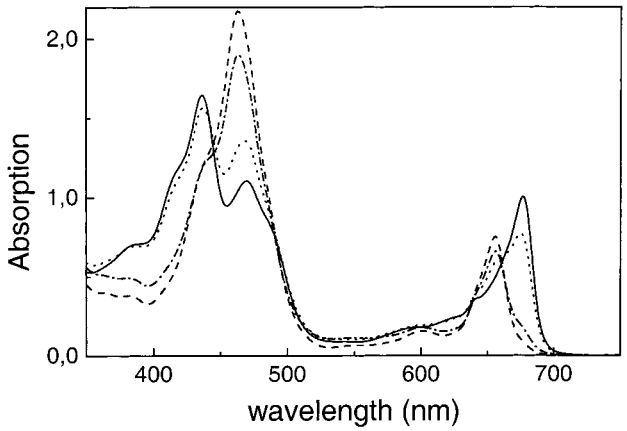

FIGURE 5: Absorption spectra at RT of reconstituted complexes with different Chl *a*/*b* ratios: rCP26-2.08 (—), rCP26-1.1 (···), rCP26-0.23 (—·—), and rCP26-0.11 (- - -). Spectra were normalized to Chl concentration as determined by pigment analysis.

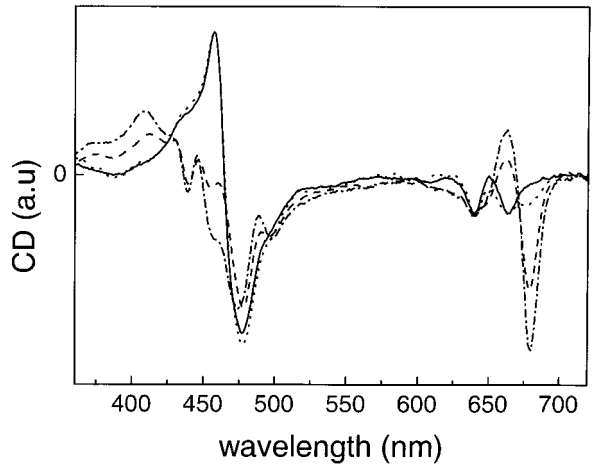

FIGURE 6: Circular dichroism spectra of complexes reconstituted with different Chl *a*/*b* ratios: rCP26-2.08 (—·—), rCP26-0.23 (···), rCP26-1.1 (- - -), and rCP26-0.11 (—). The spectra are normalized at 640 nm.

a defect in excitation energy transfer. In complexes with high Chl *b* content, the selectivity of excitation was lower due to the dominating contribution of Chl *b* absorption. Thermal equilibration was thus investigated by Stepanov analysis (*50*) (Figure 4C), confirming a Boltzmann distribution of the excited states.

Absorption spectra (RT) of selected rCP26 complexes are reported in Figure 5, upon normalization to the Chl content. By decreasing the Chl *a*/*b* ratio, we increased the amplitude of a 657 nm absorption band versus a decrease of a 679 nm component, suggesting that Chl *a* binding sites absorbing at 679 nm were readily available for Chl *b* binding which is then tuned to 657 nm absorption. A similar effect was observed in the Soret region through the decrease in the magnitude of the 436 nm component while a 462 nm peak is emerging from a 470 nm signal in rCP26-2.08, thus locating the Chl *b* S_0-S_3 transition at 462 nm.

The CD spectra of selected rCP26 complexes, normalized at 640 nm (Figure 6), exhibit dramatic changes induced by the increased Chl *b* content. The amplitude of the major 679 nm (−) signal is reduced by half when the Chl *a* content is decreased from 6 (rCP26-2.08) to 4.7 (rCP26-1.1) per polypeptide. This suggests that a readily exchangeable Chl *a* strongly contributes to this signal together with three to four other Chl *a* molecules whose step removal leads to a complete disappearance of this signal as observed in the rCP26-0.11 complex. Concomitantly, the 664 nm (+) signal rapidly disappears, revealing a negative contribution at the same wavelength which has to be ascribed to the only Chl *a* still bound to the complex and indispensable for its folding (see above). In the Soret region, the spectrum of rCP26-0.23 is dominated by a conservative signal with 478 (−) and 456 nm (+) terms, thus suggesting strong interaction between at least two Chl *b* molecules. With an increase in the amount of Chl *a* in the complex, the main negative signal shifts from 680 to 673 nm and new components at shorter wavelengths appear.

Spectral Deconvolution. The selectivity of binding sites in higher-plant antenna complexes is not equal. Some bind Chl *a*, some bind Chl *b*, and others can bind either of the two species. Four mixed sites were previously found in CP29 (*29*), and three of these were conserved in LHCII (*6*).

Assignment of mixed sites in rCP26 can be attempted on the basis of the sites' differential ability in binding either Chl *a* or Chl *b* depending on pigment availability during protein folding in vitro. Sites with high selectivity are expected to exchange their chromophore only with a strong deviation of the Chl *a*/*b* ratio in the reconstitution mixture or to remain empty. Chromophores in different binding sites can be identified on the basis of their transition energy (*6*, *29*). We have therefore analyzed the absorption spectra of rCP26 proteins with different Chl *a*/*b* ratios by deconvolution into spectral components. The deconvolution procedure that was used was strikingly different with respect to that used in previous work (*15*, *51*, *52*): spectra of Chls in a protein environment (*47*, *53*), rather than spectra of Gaussians or Chls in organic solvent, were used. We stress that the spectra of Chl in the protein environment are rather different from those in solution (*53*), showing more structure including vibrational bands, thus allowing higher stringency in the fitting procedure. Moreover, it was possible to closely feature not only the spectral shape but also the ratio of Chl *a* to Chl *b* as determined by HPLC analysis. Figure 7A reports the results obtained in the case of rCP26-2.08, showing three Chl *b* and six Chl *a* absorption forms. This is the minimal number of forms needed to closely describe the spectrum. In the best description, the three Chl *b* forms peak at 639, 648, and 656 nm, while the Chl *a* forms absorb at 662, 667, 670, 675, 679, and 681 nm. This figure is consistent with previous findings by mutation analysis of single chromophores (*6*, *29*). In the following, we used this set of forms to describe the absorption spectra of all others rCP26 complexes with different Chl *a*/*b* ratios. Whereas in this case the wavelengths were used as a fixed parameter, the distribution of the residues (not shown) for all spectra was almost identical to what was obtained in the analysis of rCP26-2.08, thus confirming that this description is a good approximation of the spectral form distribution in CP26. The results that were obtained are summarized in Figure 7B where the content in individual spectral forms of the different rCP26 preparations is shown upon normalization to the protein content, thus showing the stoichiometry of chromophores absorbing at each wavelength. It is striking that the relative amplitude of the individual spectral forms responds selectively to the changing Chl *a*/*b* ratio. In the

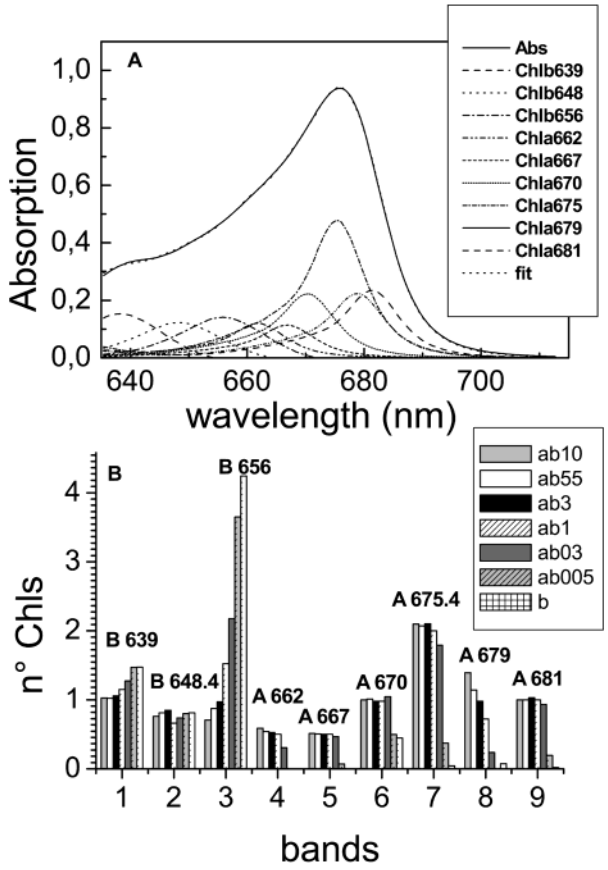

FIGURE 7: (A) Fitting of the red region absorption spectrum at RT of rCP26-2.08 with the spectra of individual Chls in a protein environment. (B) Histogram of areas for the different subbands as obtained from deconvolution of the red region (630−710 nm) of the absorption spectra of complexes with different Chl *a*/*b* ratios with the spectra of individual pigments (see the text). Spectra were normalized to protein concentration.

following, we summarize the effects on the amplitude of the different forms referring to rCP26-2.08 which has a Chl *a*/*b* ratio and absorption very similar to those of nCP26.

Chl *b* 648 did not change, indicating this absorption originates from a Chl *b* selective site.

Chl *b* 639 changed amplitude within a half-unit range, suggesting at least one site modulates its Chl *a* versus Chl *b* content. The fact that this absorption form accounts for fewer than two Chls *b* molecules, even in the presence of a large amount of Chl *b*, can be tentatively attributed to the presence of an excitonic band.

Chl *b* 656 showed the largest amplitude variations. A small increase in Chl *b* availability induced an increase by 0.5 Chl of this absorption form, suggesting mixed (Chl *a*/Chl *b*) affinity for a 656 nm site. The decrease by a similar extent induced at a higher Chl *a* content supported this conclusion. A higher Chl *b* content leads to a further increase by three Chls, implying that three sites, normally binding Chl *a*, can originate this absorption when occupied by Chl *b*. At least two of these sites are possibly located close to each other or to a site selective for Chl *b*, since a strong Chl *b*−Chl *b* excitonic interaction is produced under these conditions as detected by CD (Figure 6).

For Chl 662 and Chl 667, the low amplitude of these components (0.5 Chl/CP26) may suggest they originate from mixed sites; a decrease in the 662 nm intensity is observed for small changes in the Chl *a*/*b* ratio, while the 667 nm band only disappears at a very high Chl *b* level.

Chl 670 is the only Chl *a* form surviving high Chl *b* conditions. It is thus associated with a Chl *a* site that is indispensable for folding.

Chl 675.5 originates from at least two Chl *a* sites. One of them might be empty at a high Chl *b* level since its amplitude suddenly drops in rCP26-0.11 and CP26-0.23 which bind seven rather than nine Chls.

Chl 679 shows the typical behavior of a mixed site. Its intensity increases together with Chl *a* and decreases upon increasing Chl *b*. It can be associated with two mixed sites with similar Chl *a* and Chl *b* affinity.

Chl 681 is the red-most absorption form. It originates from a single Chl *a* binding site, which is either empty or occupied by Chl *b*, when this pigment is in excess.

Carotenoids. To study the xanthophyll binding to rCP26, the apoprotein was reconstituted in the presence of a single carotenoid species, or a combination of two. A stable complex was obtained in all cases except when neoxanthin was the only xanthophyll species available, in agreement with the case of LHCII (*7*) and CP29 (R. Bassi et al., unpublished observations). These results support the idea that neoxanthin alone is unable to stabilize Lhcb protein folding. The total number of Chls bound per polypeptide and the Chl *a*/*b* ratio of the reconstituted complexes were not affected by the occupancy of the binding sites by different xanthophyll species. However, see below about zeaxanthin binding.

It is interesting to note that when the rCP26 was reconstituted with a single xanthophyll species (lutein, violaxanthin, or zeaxanthin) or a combination of these, an exact stoichiometry of two xanthophylls per polypeptide was obtained, while the addition of neoxanthin consistently yielded complexes binding slightly more than two carotenoids (2.2−2.3) per polypeptide (Table 2). These results suggest the presence of a third xanthophyll binding site, probably specific for neoxanthin, with low affinity compared to those of the other two sites.

Table 2: Pigment Content of Samples with Different Carotenoid Compositions[a]

	Chl *a*/*b*	Chl tot	Neo	Viola	Lute	Zeaxan
rCP26-L	2.41 ± 0.03	9			1.95	
rCP26-V	2.43 ± 0.03	9		1.97		
rCP26-Z	2.0 ± 0.04	9				1.96
rCP26-LV	2.3 ± 0.03	9		1.1	0.77	
rCP26-LN	2.3 ± 0.05	9	1		1.3	

[a] The samples were named after the carotenoid species used in the reconstitution mix (e.g., rCP26-L, complex reconstituted in the presence of only lutein as a xanthophyll).

The effect of xanthophyll composition on the complex stability was studied by monitoring the decrease in the magnitude of the CD signal induced by increasing temperature. The data are summarized in Table 3. The control rCP26 protein, binding L, N, and V, and rCP26-LN show the highest melting temperature (60 °C), while samples reconstituted with violaxanthin or zeaxanthin as the only xanthophyll species showed the lowest stability (50 °C). Intermediate values were obtained for CP26-L and CP26-LV. The absorption spectra of some rCP26 with different carotenoid composition are reported in Figure 8A. Only small changes were observed in the Q_y Chl region, while larger differences

Table 3: Denaturation Temperatures of Complexes with Different Car Compositions[a]

	denaturation *T* (°C)		denaturation *T* (°C)
rCP26-2.08	60.4	rCP26-Z	49.1
rCP26-L	54.8	rCP26-LN	59.2
rCP26-V	51.8	rCP26-LV	54.4

[a] The error in the measurements can be estimated to be 2 °C.

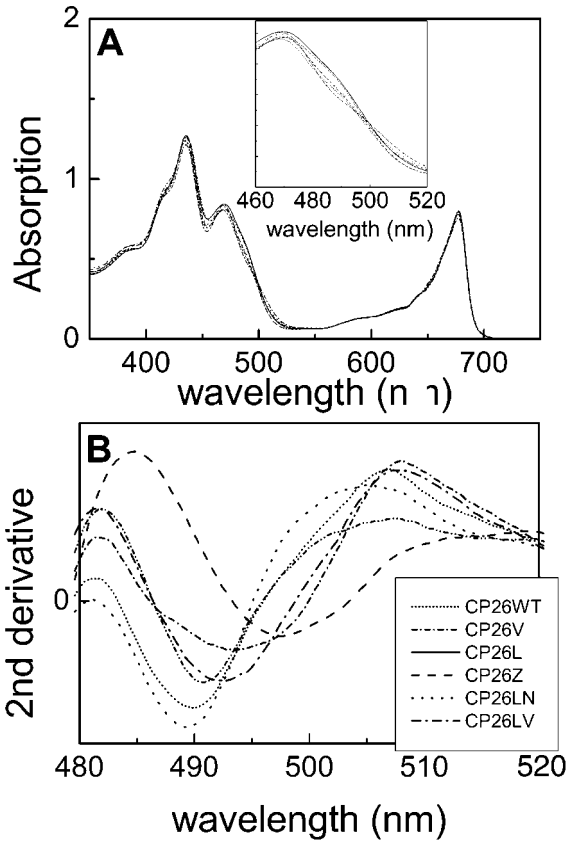

FIGURE 8: Absorption spectra at RT (A) and their second derivative (B) of reconstituted complexes with different carotenoid compositions: (—) CP26-LVN, (– – –) CP26-V, (•••) CP26-L, (—•—) CP26-Z, (—••—) CP26-LN, and (- - -) CP26-LV. The inset in panel A highlights the absorption region in which car absorbs. Spectra were normalized to Chl concentration as determined by pigment analysis.

were present in the Soret region from direct Cars absorption as detected by second-derivative analysis in the 480−510 nm range (Figure 8B) where the red-most peak of xanthophyll S_0-S_2 transitions can be resolved (*7*). The second derivatives of rCP26-LNV, CP26-LN, and rCP26-L spectra show a minimum at 490−491 nm, which can thus be associated with lutein absorption. Two contributions were resolved in rCP26-V (492 and 498 nm) and CP26-LV (491 and 497 nm). rCP26-Z binds the red-most xanthophylls with absorptions at 498 and 503 nm. These results indicate that xanthophylls absorb at different wavelength depending on the site to which they are bound. This is in agreement with previous results with LHCII (*23*).

The Q_y and Soret spectral regions were further analyzed by CD spectroscopy in investigating the effect of modified occupancy of xanthophyll binding sites on pigment organization (Figure 9). The major effect, consisting of a shift of the Chl *b* (−) signal from 640 to 648 nm, was obtained in proteins lacking neoxanthin. This effect is complete in

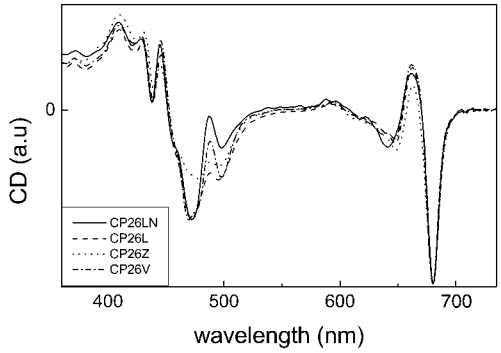

FIGURE 9: Circular dichroism spectra of complexes reconstituted with different carotenoid compositions: rCP26-LN (—), rCP26-L (- - -), rCP26-Z (•••), and rCP26-V (—•—). Spectra were normalized to Chl concentration as determined by pigment analysis.

rCP26-Z and in rCP26-L samples where the 640 nm signal disappears. In the Soret region, a dramatic effect is observed on the amplitude of the 473 nm (−) signal, the magnitude of which is strongly decreased in rCP26-Z where two signals at 471 and 478 nm appear. The amplitude of the 495 nm (−) signal is also strongly affected by changing xanthophyll binding. Its amplitude was minimal in rCP26-3 and rCP26 LN samples, and it was increased by any modification of xanthophyll composition. It is possible that this apparent increase in the magnitude of the 495 nm (−) signal actually originates from the disappearance of a superimposing 488 nm (+) signal which is only apparent in the spectra of CP26 complexes binding neoxanthin. This would further support the view that neoxanthin organization is different in CP29 and CP26 with respect to LHCII (see Figure 3).

DISCUSSION

The determination of the method of chromophore binding to the individual sites is of primary importance for the understanding of the structure and function of Lhc proteins. However, this task is particularly difficult due to the overlapping of the absorption from multiple Chl *a* and Chl *b* ligands. Further complication comes from part of the sites binding Chl *a* or Chl *b*, thus generating additional spectral complexity. Characterization of each of the 17 binding sites in LHCII and of the 10 binding sites in CP29 has been accomplished by mutation analysis (*6*−*8*, *29*, *49*, *54*), leading to modeling of energy transfer in Lhc proteins (*3*, *24*, *55*). Similar studies need to be extended to other members of the Lhc protein family, to clarify the functional implications of the differences in primary structure and pigment binding. In this study, we have investigated the properties of the different binding sites by changing their occupancy. The characteristics of each chromophore-binding site were assigned on the basis of spectroscopic and biochemical measurements. Previous work showed that in CP29 a subset of the binding sites present in LHCII was conserved, namely, Chl sites A1−A5, B3, B5, and B6 and xanthophyll binding sites L1 and L2 (*29*). In the following, we compare the properties of the different domains of CP26 which can be spectrally defined, with the corresponding domains of CP29 and LHCII with the aim of defining which pigment binding sites are conserved and to identify differences.

All the amino acid residues which are Chl ligands in CP29 are conserved in CP26, with the exception of the A2 ligand:

His in CP29 versus Asn in CP26. This is a conservative substitution since asparagine was shown to be the ligand of Chl A2 in LHCII (*6*, *31*). Consistent with the primary sequence homology, the pigment binding properties of CP26 and CP29 are similar, except for one additional Chl *b* that is present in CP26 but not in CP29.

The Additional Chl b in CP26. The major spectral difference between CP26 and CP29 is the presence of an absorption band at 648−650 nm, which is thus likely to represent the contribution of the additional Chl *b* detected by pigment analysis. This is consistent with the results of spectral deconvolution (Figure 7B), showing a 648 nm band being conserved with changing the Chl *b* content. This indicates that the additional Chl *b* present in CP26 is bound to a Chl *b* selective site, while all the Chl *b* molecules in CP29 were shown to be located in promiscuous sites. Differences in CD spectra can be used to identify the CP26 domain hosting this Chl *b*. The 664 nm signal has zero amplitude in CP29, while it is clearly positive in both CP26 and LHCII. Mutation analysis on LHCII showed a decrease in the magnitude of this signal when the Chl A2 ligand is removed, which leads to the loss of Chl A2 and B2. This was shown to be due to the removal of an excitonic interaction between Chl A4 and A2, mediated by Chl B2 (*6*). In CP29, lacking Chl B2, the same mutation does not affect this spectral region. This suggests that the 664 nm (+) signal is related to the occupancy of the Chl B2 site. The presence of this signal in CP26 thus implies the occupancy of site B2.

It can be asked why CP26 binds Chl B2 while CP29 cannot. We suggest this is because Chl A2 is bound by different ligands. Both asparagine and histidine can coordinate Chl A2 (*6*, *29*), but binding through asparagine appears to allow further coordination of Chl B2 through Chl A2 by a yet unknown mechanism. We propose that Chl A2, when coordinated by histidine, may assume an orientation different from that induced upon coordination by asparagine. This is supported by LD spectroscopy. In LHCII, which coordinates Chl A2 through an asparagine side chain, this chromophore is the major source of the red-most positive LD signal (R. Bassi, R. Croce, and J. Breton, unpublished results), while A2 in CP29 makes a much smaller contribution (*49*), implying a different orientation of Chl A2.

A Chl a Is Essential for Protein Folding. The refolding of CP26 in the presence of limiting amounts of Chl *a* yields a complex with a single bound Chl *a* which is essential for folding. Recent work showed that Chl A1 is the only chlorophyll essential for protein folding in LHCII (*56*) and CP29 (*29*). It is striking to conclude that the only residual Chl *a* in rCP26<001 is bound to site A1. Analysis of the absorption spectrum of rCP26-0.11 in terms of absorption of individual pigments (Figure 10) shows a single Chl *a* absorption at 671 nm. This is consistent with the previous attribution of Chl A1 absorption at 669 nm in CP29 (*29*).

Selectivity of Chlorophyll Binding Sites. Figure 11 shows a model for the occupancy of Chl binding sites in CP26 based on CP29 with the addition of Chl B2. The next step is to assign each site to Chl *a*, to Chl *b*, or to mixed occupancy. The selectivity of binding sites is not equal among Lhc proteins. Four mixed sites were previously found in CP29 (*29*), two of which (sites A3 and B3) were conserved among three in LHCII (*6*). Since the C-terminal domain, including

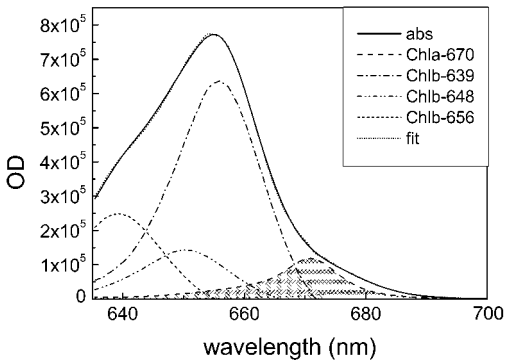

FIGURE 10: Fitting of the red region absorption spectrum at RT of rCP26-0.11 with the spectra of individual Chls in a protein environment. The filled spectrum represents the absorption form of the only Chl *a* present in this complex.

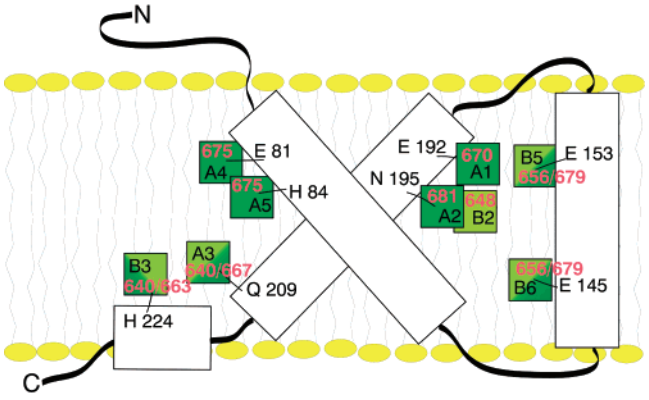

FIGURE 11: Schematic drawing of the pigment organization and absorption of CP26. The color filling in the representation of the Chls indicates the side occupancy: dark green for Chl *a* and light green for Chl *b*. The mixed site occupancy is represented by the presence of the two colors.

A3 and B3 ligands, is strongly conserved among the three Lhc proteins, we propose that in CP26 sites A3 and B3 have mixed occupancy.

The CP26 minus CP29 difference absorption spectrum (Figure 1C) shows a conservative signal, with 662 (+) and 679 nm (−) terms, indicating a blue shift of a Chl *a* form. This shift may originate from differences in the distribution of polar residues in the close surroundings of the Chl B3 His ligand, consistent with sequence comparison (not shown). The Chl *a* absorption component of site B3 was identified at 679 nm in CP29, while it was at 665 nm in LHCII (*6*, *29*). We propose that Chl *a* in site B3 of CP26 absorbs around 662 nm, thus fitting the shift of the CP26 minus CP29 difference spectrum. The Chl *b* contribution of site B3 of CP26 is expected to be similarly shifted. This can be appreciated at cryogenic temperatures (Figure 1B). We conclude that site B3 of CP26 is a mixed site yielding 662 nm Chl *a* and 640 nm Chl *b*, in agreement with the results of spectral deconvolution (Figure 7B).

Mutation analysis on LHCII and CP29 showed that the affinity of site B6 for Chl *a* versus Chl *b* is modulated by the ligand residue. It only binds Chl *b* in wild-type LHCII through Gln131 but is switched to a mixed site in the Glu131 mutant. Consistently, wild-type CP29 binds both Chl *a* and *b* through Glu166 but only Chl *b* in the Gln166 mutant (*29*). CP26 bears a Glu in the corresponding (145) position, suggesting B6 is a mixed site. This is supported by the

spectral analysis of rCP26 with an altered Chl *a*/*b* ratio (Figure 7B), showing a mixed site with 679 (Chl *a*) and 656 nm (Chl *b*) contributions. Similar spectral features have been associated with site B6 in CP29.

Analysis of the absorption spectra of rCP26 complexes with different Chl *a*/*b* ratios shows that the amplitudes of three absorption forms (670, 675, and 681 nm), accounting for four Chls, do not respond to small changes in the Chl *a*/*b* ratio, thus suggesting the presence of four sites selective for Chl *a* in control CP26. The amplitude of two additional Chl *a* forms (Chl 662 and Chl 667) accounts for less than one Chl per polypeptide. Consistently, we propose these represent the Chl *a* contribution of sites with mixed Chl *a*/Chl *b* occupancy (*29*).

The amplitude of the last Chl *a* spectral form (679 nm), which accounts for one Chl *a* per polypeptide in rCP26-2.08, shows a strong dependence upon small changes in the Chl *a*/*b* ratio, suggesting it rather derives from two Chl *a* contributions from mixed sites. This figure, which implies for CP26 the presence of four Chl *a* specific sites and one Chl *b* specific site and four more sites with mixed occupancy, although tentative, is supported by the strong spectroscopic and biochemical similarity between CP29 and CP26. In CP29, sites A1 (669 nm), A2 (680 nm), A4 (676 nm), and A5 (675 nm) are specific for Chl *a*. The attribution of the 670 nm absorption in CP26 to Chl A1 is supported by its presence in rCP26 with the single Chl *a* needed for pigment−protein assembly (see above). Chl A2 can be associated with the 681 nm absorption because this is the red-most absorbing Chl in both CP29 and LHCII (*6*, *29*). On a similar basis, we can associate the 675 nm absorption form, accounting for two Chls, with sites A4 and A5.

Four mixed sites have been identified in CP29: A3, B3, B5, and B6. Chl *a* absorbs at 668 nm in site A3, while site B5 accommodates a 678 nm Chl *a*. We can thus tentatively attribute the 667 nm form to Chl *a* in site A3 and the 679 nm form to Chl *a* in site B5. Figure 11 summarizes the above discussion in a schematic model of Chl organization in CP26, which is supported by the strong spectroscopic similarity between the two pigment−protein complexes except for the Chl *b* 648 nm component, which needs to be confirmed by future experiments.

Carotenoid Binding Sites. Reconstitution experiments in the presence of different carotenoid species indicate that CP26 tightly binds two xanthophylls per polypeptide, in agreement with the data from nCP26 purified from thylakoids. Both sites can accommodate lutein and violaxanthin or zeaxanthin, while neoxanthin can enter only one. The location of each xanthophyll species within CP26 can be proposed by comparison with CP29 and LHCII. Three high-affinity binding sites have been reported in Lhc proteins: L1 and L2 cross bracing helices A and B (*5*) and N1, close to helix C (*54*). Occupancy of site L1 was shown to be indispensable for protein folding in LHCII (*56*), while neoxanthin was unable to sustain folding in Lhc proteins (*15*, *36*, *46*, *54*), implying it must bind to either site L2 or N1. It was shown that LHCII can fold in the absence of neoxanthin both in vivo and in vitro (*7*, *48*, *57*) without a decrease in stability. In CP26, binding of neoxanthin significantly increases the heat stability of the complex, suggesting it binds to site L2. This is consistent with two previous findings. (i) LHCII decreases its stability to heat denaturation when the L2 site is empty, and (ii) neoxanthin is located in site L2 of CP29 (*29*). Violaxanthin complements to one molecule per polypeptide with neoxanthin, suggesting it also binds to site L2. Lutein was shown to occupy site L1 in both CP29 and LHCII, although it can also bind to site L2 in the absence of violaxanthin.

We conclude that the xanthophyll location and distribution in CP26 are very similar to those in CP29 with lutein in site L1 and violaxanthin or neoxanthin in site L2. This is different with respect to LHCII for the location of neoxanthin. It should be mentioned that we observed slightly more than two carotenoids per polypeptide upon refolding with neoxanthin. This may suggest the presence of a third car-binding site, with low affinity and high selectivity for neoxanthin. It was recently shown that the neoxanthin site has a decreased affinity in Lhcb3, a LHCII component lacking the Chl binding site A7 (*58*). Since neoxanthin was shown to bind to LHCII through interaction with Chls (*7*), it might be that CP26, lacking not only Chl A7 but also Chl A6 and Chl B1 in the helix C domain, has a neoxanthin binding site with even lower affinity. Phylogenetic analysis shows a strong relation between Lhcb3 and Lhcb5 (CP26) (*59*). Since even the mildest solubilization yields a release of neoxanthin, we cannot exclude the possibility that CP26 might bind an additional molecule of neoxanthin in vivo.

CD spectra of rCP26 incorporating different xanthophyll species only show small changes, except in the case of zeaxanthin binding. In this case, the major signal in the Soret region at 473 nm (−) disappears and the Chl *b* signal in the Q_y region, 648 nm (−), undergoes an 8 nm blue shift. This might be related to the recent work (*4*) showing that incorporation of zeaxanthin into site L2 of Lhc proteins promotes a conformational change to a dissipative state characterized by short-living fluorescence emission. In vivo, CP26 undergoes exchange of violaxanthin with zeaxanthin under high-light conditions (*34*, *60*), while the recombinant protein incorporating zeaxanthin has a lower fluorescence yield (*28*). The large CD change detected strongly suggests conformational changes involving reorganization of pigment−pigment interactions within CP26. Work is in progress for clarifying if the CD change is related to the mechanism of fluorescence quenching.

ACKNOWLEDGMENT

We thank Dr. Jacques Breton for LD spectra, helpful discussion, and careful reading of the manuscript and Stefano Caffarri for the programs of spectra analysis and fitting. R.C. thanks Prof. Emilio Burattini.

REFERENCES

1. Jansson, S. (1999) *Trends Plant Sci. 4*, 236−240.
2. Bassi, R., and Caffarri, S. (2000) *Photosynth. Res. 64*, 243−256.
3. Van Amerongen, H., and van Grondelle, R. (2001) *J. Phys. Chem. B 105*, 604−617.
4. Moya, I., Silvestri, M., Vallon, O., Cinque, G., and Bassi, R. (2001) *Biochemistry 40*, 12552−12561.
5. Kühlbrandt, W., Wang, D. N., and Fujiyoshi, Y. (1994) *Nature 367*, 614−621.
6. Remelli, R., Varotto, C., Sandona, D., Croce, R., and Bassi, R. (1999) *J. Biol. Chem. 274*, 33510−33521.
7. Croce, R., Weiss, S., and Bassi, R. (1999) *J. Biol. Chem. 274*, 29613−29623.

8. Caffarri, S., Croce, R., Breton, J., and Bassi, R. (2001) *J. Biol. Chem. 276*, 35924−35933.
9. Mullet, J. E. (1983) *J. Biol. Chem. 258*, 9941−9948.
10. Testi, M. G., Croce, R., Polverino-De Laureto, P., and Bassi, R. (1996) *FEBS Lett. 399*, 245−250.
11. Pesaresi, P., Sandona, D., Giuffra, E., and Bassi, R. (1997) *FEBS Lett. 402*, 151−156.
12. Walters, R. G., Ruban, A. V., and Horton, P. (1996) *Proc. Natl. Acad. Sci. U.S.A. 93*, 14204−14209.
13. Jegerschöld, C., Rutherford, A. W., Mattioli, T. A., Crimi, M., and Bassi, R. (2000) *J. Biol. Chem. 275*, 12781−12788.
14. Dainese, P., and Bassi, R. (1991) *J. Biol. Chem. 266*, 8136−8142.
15. Pagano, A., Cinque, G., and Bassi, R. (1998) *J. Biol. Chem. 273*, 17154−17165.
16. Croce, R., and Bassi, R. (1998) in *Photosynthesis: Mechanisms and Effects* (Garab, G., Ed.) pp 421−424, Kluwer Academic Publishers, Dordrecht. The Netherlands.
17. Plumley, F. G., and Schmidt, G. W. (1987) *Proc. Natl. Acad. Sci. U.S.A. 84*, 146−150.
18. Paulsen, H., Finkenzeller, B., and Kuhlein, N. (1993) *Eur. J. Biochem. 215*, 809−816.
19. Giuffra, E., Cugini, D., Croce, R., and Bassi, R. (1996) *Eur. J. Biochem. 238*, 112−120.
20. Kleima, F. J., Gradinaru, C. C., Calkoen, F., van Stokkum, I. H. M., van Grondelle, R., and Van Amerongen, H. (1997) *Biochemistry 36*, 15262−15268.
21. Gradinaru, C. C., Özdemir, S., Gülen, D., van Stokkum, I. H. M., van Grondelle, R., and Van Amerongen, H. (1998) *Biophys. J. 75*, 3064−3077.
22. Agarwal, R., Krueger, B. P., Scholes, G. D., Yang, M., Yom, J., Mets, L., and Fleming, G. R. (2000) *J. Phys. Chem. B 104*, 2908−2918.
23. Croce, R., Muller, M. G., Bassi, R., and Holzwarth, A. R. (2001) *Biophys. J. 80*, 901−915.
24. Cinque, G., Croce, R., Holzwarth, A. R., and Bassi, R. (2000) *Biophys. J. 79*, 1706−1717.
25. Young, A. J., Phillip, D., Ruban, A. V., Horton, P., and Frank, H. A. (1997) *Pure Appl. Chem. 69*, 2125−2130.
26. Ruban, A. V., Young, A. J., and Horton, P. (1996) *Biochemistry 35*, 674−678.
27. Crimi, M., Dorra, D., Bosinger, C. S., Giuffra, E., Holzwarth, A. R., and Bassi, R. (2001) *Eur. J. Biochem. 268*, 260−267.
28. Frank, H. A., Das, S. K., Bautista, J. A., Bruce, D., Vasil′ev, S., Crimi, M., Croce, R., and Bassi, R. (2001) *Biochemistry 40*, 1220−1225.
29. Bassi, R., Croce, R., Cugini, D., and Sandona, D. (1999) *Proc. Natl. Acad. Sci. U.S.A. 96*, 10056−10061.
30. Yang, C. H., Kosemund, K., Cornet, C., and Paulsen, H. (1999) *Biochemistry 38*, 16205−16213.
31. Rogl, H., and Kuhlbrandt, W. (1999) *Biochemistry 38*, 16214−16222.
32. Boekema, E. J., van Roon, H., Calkoen, F., Bassi, R., and Dekker, J. P. (1999) *Biochemistry 38*, 2233−2239.
33. Ruban, A. V., Lee, P. J., Wentworth, M., Young, A. J., and Horton, P. (1999) *J. Biol. Chem. 274*, 10458−10465.
34. Bassi, R., Pineau, B., Dainese, P., and Marquardt, J. (1993) *Eur. J. Biochem. 212*, 297−303.
35. Sandona, D., Croce, R., Pagano, A., Crimi, M., and Bassi, R. (1998) *Biochim. Biophys. Acta 1365*, 207−214.
36. Ros, F., Bassi, R., and Paulsen, H. (1998) *Eur. J. Biochem. 253*, 653−658.
37. Ruban, A. V., Young, A. J., Pascal, A. A., and Horton, P. (1994) *Plant Physiol. 104*, 227−234.
38. Walters, R. G., Ruban, A. V., and Horton, P. (1994) *Eur. J. Biochem. 226*, 1063−1069.
39. Berthold, D. A., Babcock, G. T., and Yocum, C. F. (1981) *FEBS Lett. 134*, 231−234.
40. Dainese, P., Hoyer-Hansen, G., and Bassi, R. (1990) *Photochem. Photobiol. 51*, 693−703.
41. Gilmore, A. M., and Yamamoto, H. Y. (1991) *Plant Physiol. 96*, 635−643.
42. Hirs, C. H. W. (1967) *Methods Enzymol. 11*, 325−329.
43. Zucchelli, G., Dainese, P., Jennings, R. C., Breton, J., Garlaschi, F. M., and Bassi, R. (1994) *Biochemistry 33*, 8982−8990.
44. Haworth, P., Arntzen, C. J., Tapie, P., and Breton, J. (1982) *Biochim. Biophys. Acta 679*, 428−435.
45. Haworth, P., Tapie, P., Arntzen, C. J., and Breton, J. (1982) *Biochim. Biophys. Acta 682*, 152−159.
46. Giuffra, E., Zucchelli, G., Sandona, D., Croce, R., Cugini, D., Garlaschi, F. M., Bassi, R., and Jennings, R. C. (1997) *Biochemistry 36*, 12984−12993.
47. Cinque, G., Croce, R., and Bassi, R. (2000) *Photosynth. Res. 64*, 233−242.
48. Connelly, J. P., Müller, M. G., Bassi, R., Croce, R., and Holzwarth, A. R. (1997) *Biochemistry 36*, 281−287.
49. Simonetto, R., Crimi, M., Sandona, D., Croce, R., Cinque, G., Breton, J., and Bassi, R. (1999) *Biochemistry 38*, 12974−12983.
50. Stepanov, B. I. (1957) *Sov. Phys. Dokl. 2*, 81−84.
51. Hemelrijk, P. W., Kwa, S. L. S., van Grondelle, R., and Dekker, J. P. (1992) *Biochim. Biophys. Acta 1098*, 159−166.
52. Trinkunas, G., Connelly, J. P., Müller, M. G., Valkunas, L., and Holzwarth, A. R. (1997) *J. Phys. Chem. B 101*, 7313−7320.
53. Zucchelli, G., Jennings, R. C., Garlaschi, F. M., Cinque, G., Bassi, R., and Cremonesi, O. (2002) *Biophys. J. 82*, 378−390.
54. Croce, R., Remelli, R., Varotto, C., Breton, J., and Bassi, R. (1999) *FEBS Lett. 456*, 1−6.
55. Iseri, E., and Gulen, D. (2001) *Eur. Biophys. J. 30*, 344−353.
56. Formaggio, E., Cinque, G., and Bassi, R. (2001) *J. Mol. Biol. 314*, 1157−1166.
57. Hobe, S., Niemeier, H., Bender, A., and Paulsen, H. (2000) *Eur. J. Biochem. 267*, 616−624.
58. Caffarri, S., Croce, R., Cattivelli, L., and Bassi, R. (2002) *PS2001 Proceedings*, CSIRO Publishing (in press).
59. Bassi, R., Giuffra, E., Croce, R., Dainese, P., and Bergantino, E. (1996) in *Life Science* (Jennings, R. C., Zucchelli, G., Ghetti, F., and Colombetti, G., Eds.) NATO ASI Series 287, pp 41−63, Plenum Press, New York.
60. Ruban, A. V., and Horton, P. (1994) *Photosynth. Res. 40*, 181−190.

BI0257437